Journal of Materials Chemistry C

Accepted Manuscript

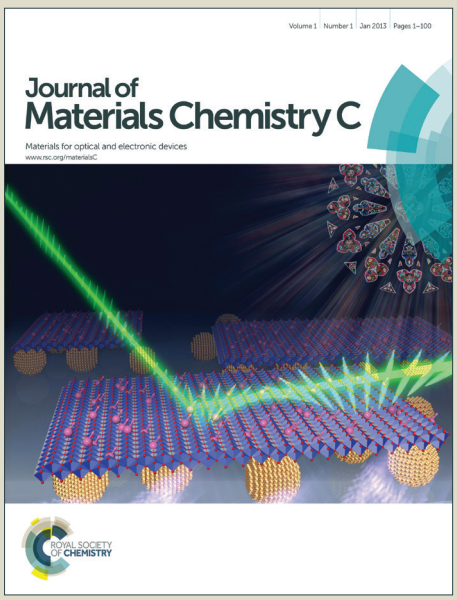

ROYAL SOCIETY OF CHEMISTRY

www.rsc.org/materialsC

Journal of
Materials Chemistry C

RSCPublishing

COMMUNICATION

Reducing the effects of shot noise using nanoparticles†

Cite this: DOI: 10.1039/x0xx00000x

Moshood K. Morakinyo[b] and Shankar B. Rananavare*[a]

Received ooth January 2012,
Accepted ooth January 2012

DOI: 10.1039/x0xx00000x

www.rsc.org/

Abstract: We present a hybrid nano-lithographic approach to minimizes the effects of line edge roughness and shot noise in nano-hole patterning by reflowing photoresist polymers around the nanoparticles deposited using self-assembly and simple etch chemistries. The method extends the transistor contact holes patterning limits to below 20 nm.

The path of the semiconductor industry set up by Moore's power law[1] has been paved through major breakthroughs in lithography. The work-horse of modern top-down patterning is optical lithography wherein the pattern resolution is directly proportional to the wavelength and inversely proportional to the numerical aperture, NA, of the exposure system. The resolution has been progressively improved through use of excimer lasers, phase shift masks[2], and even immersion[3] in liquids to increase NA > 1. Currently viable paths to 20 nm node and beyond include extreme UV sources (λ =13 nm) or double and quadruple patterning techniques of multilayer resist processing of high complexity[4, 5].

At nanometer length scales, shot noise effects arising from statistical fluctuations in number of photons arriving within nanoregion lead to fluctuations in final dimensions of the patterned structure. These effects are more pronounced in high energy (low photon/particle count) EUV and, E-beam exposure systems[6]. Additionally, supersensitive chemically amplified (quantum efficiency > 1) photoresists, introduce a chemical shot noise caused by deviation in the number of photo-reactive molecules in exposed nanoregions. Such effects may be suppressed with lower sensitivity resists needing longer exposures, which reduces throughput. On molecular scale, the line edge roughness contribution arising from the polymer size used in photoresists may be reduced by lower molecular weight polymers and ultimately through use of molecular resists[7]. A complementary approach to nano-patterning is through the so-called bottom up methods[8, 9] that rely on specific directed self-assembly of diblock polymers[10]. Herein the ability to direct nucleation and create nonuniform spacings, amongst desired patterns (e.g. holes or lines), remains challenging. The size distribution of molecular components [11, 12] also limits the scale and yield of fabrication [13, 14].

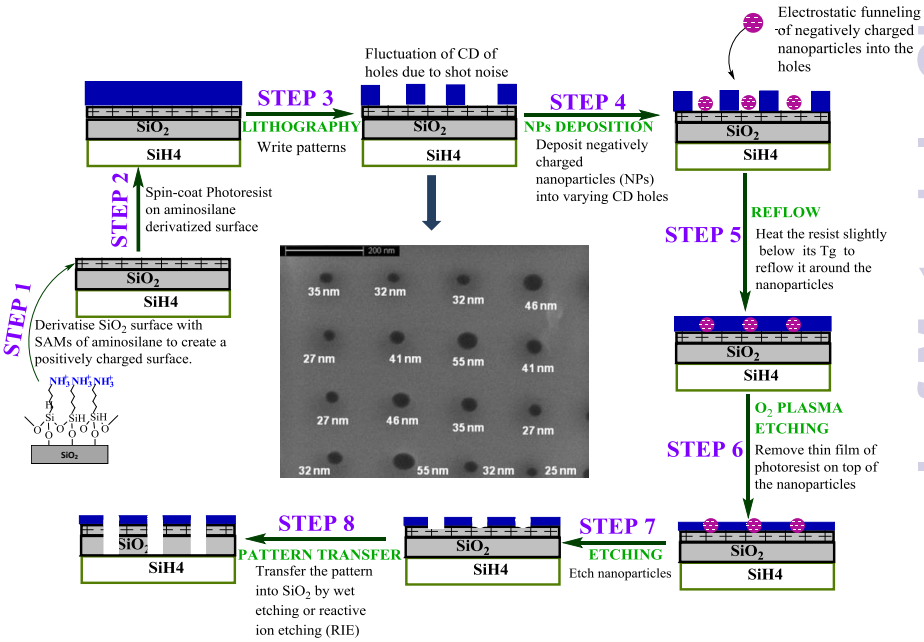

Figure 1 Schematic representation of the strategy to remove effects of shot noise and line-edge roughness for contact hole patterning using NPs of precise size. Here, critical dimension (CD) is the desired dimension of the holes. Approach (Step 1) begins with depositing a self-assembled monolayer (SAM) of silane molecule bearing positively charged amine groups on the oxide surface of a silicon wafer. Next, E-beam

lithographic is used to pattern holes (Steps 2and 3) in poly-methyl methacrylate (PMMA) photoresist film (blue layer) 2) which generates shot noise as illustrated (in SEM pattern). It exposes amine groups at the bottom of the holes. Step 4 entails aqueous phase deposition of controlled-size, citrate-capped (negatively charged) gold nanoparticles (GNPs) in lithographically patterned holes using electrostatic funneling (EF). In step 5, the PMMA is reflown around pre-deposited nanoparticles by heating wafer to 100 °C (below its glass transition temperature, 110 °C) which engulfs nanoparticles. The hole-size corresponding to the GNP dimension is recovered by oxygen plasma etching (Step 6) to expose the GNPs followed by wet etching (iodine) of GNPs (Step7). Pattern transfer in SiO_2 (Step 8) can be achieved by reactive ion etching or wet etching[15].

In this paper we present initial studies of a new hybrid approach (Figure 1) that combines the classic top-down projection lithography with electrostatically directed self-assembly to reduce effect of SN/LER. Positively charged amine groups of self-assembled-monolayers (SAMs) of AATMS (N-(2-Aminoethyl)-11-Amino-undecyl-methoxy-silane) underlying the PMMA film are exposed after development. Negatively charged PMMA resist film electrostatically funnels citrate capped negatively charged gold nanoparticles (GNPs)[16-19] into shot noise affected holes. After PMMA resist reflow, pre-deposited nanoparticles are engulfed in the resist film. They are not dislodged from the binding site owing to the strong interaction between oppositely charged GNPs and amine groups on substrate. Resist reflow step keeps the relative location of GNPs intact but erases the hole size information and with it the effects of SN/LER. The holes of GNP-size are regenerated by plasma/wet etching and their pattern is transferred in SiO_2 hard-mask layer by reactive ion etching[20]. The method relies on using better size uniformity of nanoparticles compared to a patterned nanohole (NH), i.e., $\sigma_{GNP} < \sigma_{NH}$. Here, we focus on steps (4 & 5) involving deposition of nanoparticles from solution and resist reflow around them to assess advantages and limitations of the method. Both the steps are in principle scalable to larger size substrates and do not require extensive modification of current VLSI/CMOS process flow.

First control experiment to consider is the minimum spacing between deposited nanoparticles on the unpatterned wafer surface; and how/if it depends on the dimensions of NPs. From steric packing consideration, GNPs deposited on unpatterned SAM coated surface can be described by particle density, S, which scales as, $S(N/\mu m^2) \approx \alpha/(2a+\beta l_d)^2$ where a and l_d are particle radius and Debye screening lengths respectively (Figure 2a). α and β are scaling constants. The l_d term qualitatively accounts for the inter-particle electrostatic repulsion. Thus, average spacing between the particles (effective pitch) varies as $P^U\ (nm) = 10^3/\sqrt{S}$. . Experimentally, we observe the ratio $P^U/2a$ does not depend on $2a$ but it decreases from ≈ 2 with decrease in the Debye length (hence pH/ ionic strength) reaching about 1.6 near the GNP coagulation limit (50 mM salt concentration). In the absence of electrostatic interactions, the steric packing limit for $P^U/2a$ is ≈ 1. Similarly, at the fixed ionic strength employed in Figure 2a, the ratio of net surface area of deposited nanoparticles ($S4\pi a^2$) to the unit surface area of the substrate is also constant (≈ 0.8, see inset) regardless of the diameter of GNPs implying that surface charge densities (ρ_i) for GNPs and SAM ($\rho_{SAM}/\rho_{GNP} \approx 0.8$) are similar. Other important consideration for deposition process is the selective placement of particles in holes. i.e., the particles should not deposit on the unpatterned polymer (PMMA) resist surface. The minimum thickness/screening length of the resist film, from data in Figure 2b, is ≈ 30 nm. Therefore, 30 nm or higher thickness resist film prevents deposition of negatively charged NP's on the PMMA surface that covers the positively charged SAM film.

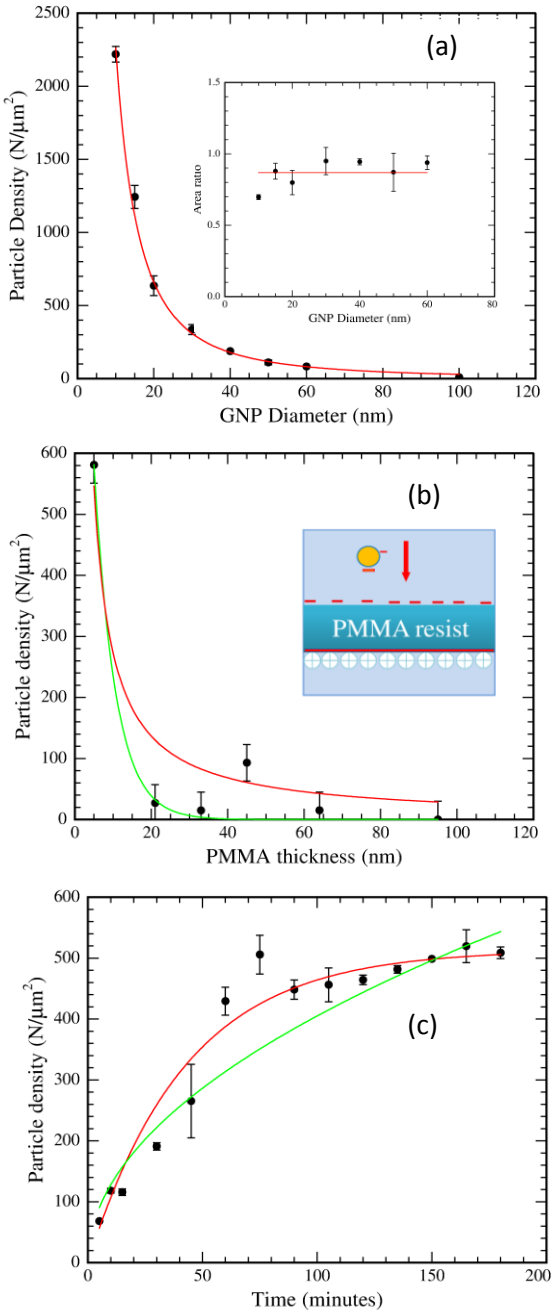

Figure 2 Particle deposition density on AATMS derivatized silicon wafer. a) Deposited particle density, $S \approx \alpha/(2a+\beta.l_d)^2$ with α =(3.11 ± 0.03) ×10^5 N, β = 0.44 ± 0.02, Debye length l_d = 4 nm, and GNP radius, a. Line (red) is a best fit. The inset shows area ratio, net area of nanoparticles deposited/μm² area of substrtate, is independent of particles size. (b) Resist film thickness (z) dependence of S follows a simple a_1/z (red) or $a_2 exp(-a_3 z)$(green) dependence with best fit values of are: a_1 = 2.735±0.005×10^3 N/ nm, a_2 = 1.430 ±0.0 14 ×10^3 N/ nm and a_3 = 0.181±0.002 nm^{-1} c) Time dependence of deposition for 20 nm size GNPs on AATMS derivatized surface. The red line corresponds to irreversible adsorption model $S(t) = S_0\ (1-exp(-b.t))$ with S_0 = 523 ± 2 N/um² and b =2.04 ± 0.02 ×10^2.min^{-1} While the green line is fit to $S(t) = a_4.t^{1/2}$ with a_4 = 40.8 ± 0.1 N/um²-$min^{1/2}$.

Typical time needed for solution phase deposition, as shown in Figure 2c, is 3 hours which can be reduced by increasing nanoparticle concentration; although studies reported here employ 24 hour deposition time (see below).

Figure 3 shows deposition in patterned holes driven by electrostatic funneling (3a) resulting in about 1 particle per hole (3b, left top inset) as observed by others[16]. Particle distribution around the center of holes is Gaussian (3b,top right inset). Given the small number of particles deposited per hole, a Poisson statistics is obeyed for the fill fraction determined after 24 hours of deposition time, as shown in the inset of Figure 3c. Further optimization of deposition time, NP concentration as well as surface charge densities of SAM/Resist would be needed to (1) deposit 1 particle/hole while suppressing multiple particle or lack of deposition in hole, and (2) better centering in nanoholes by enhanced electrostatic funneling.

The average number of particles deposited as a function of hole diameter (by fixing pitch) show a linear dependence with an unique diameter of 30 nm beyond which NP are not inserted in the holes. We rationalize this critical hole radius, r^{C}_{SAM} (Figure 3c) by considering charge densities ρ_{SAM} and ρ_{PMMA} and their opposite signs[21]. Postulating that negatively charged GNPs do not deposit in holes when the solution exposed wafer surface acquires net negative charge, r^{C}_{SAM} can be estimated:

$$r^{C}_{SAM} = \frac{\rho_{PMMA}\, z}{\rho_{PMMA}+\rho_{SAM}}\left(1+\sqrt{1+\theta}\right) \quad \theta = \frac{P^2(\rho_{PMMA}+\rho_{SAM})}{\pi\rho_{PMMA}\, z^2}$$

$$r^{C}_{SAM} = \sqrt{\frac{\rho_{PMMA}}{\pi(\rho_{PMMA}+\rho_{SAM})}}\,P \quad \theta >> 1$$

Here z is the photoresist film thickness. The model predicts a film thickness (z) independent r^{C}_{SAM} that is proportional to pitch (P) for θ >> 1, i.e., when $(z/P)^2$ << 1, a condition realized in our experiments; P = 200 nm, z = 30 nm. Similar results have been observed in situations where z = 0, and negatively charged SiO_2 surfaces surround the positively charged patterned holes [21].

According to the model, r^{C}_{SAM} can be reduced by decreasing the pitch or the charge density ratio, ρ_{PMMA}/ρ_{SAM}. The latter could be adjusted by pH or ionic strength of the depositing solution. Thus, these deposition studies of GNPs on unpatterned and patterned surfaces (i.e., r^{C}_{SAM}/P ratio) yield crude estimates of charge density ratios, ρ_{SAM}/ρ_{GNP} = 0.8, ρ_{PMMA}/ρ_{SAM} = 0.018 respectively. Using experimental citrate capped GNP charge density [22, 23], $\rho_{GNP} \approx$ -7.5 × 10^{14} charges/cm^2 one obtains ρ_{SAM}, ρ_{PMMA} = 6 × 10^{14} and 1.1 × 10^{13} charges/cm^2 respectively, comparable to the reported values in literature within an order of magnitude[24, 25]. A densely packed SAM, with a molecular cross-sectional area of 25Å^2 and with two positively charged amine groups on AATMS molecule yields ρ_{SAM} = 8×10^{14} charges/cm^2. Pitch, hole diameter, pH/ionic strength may be tuned to reduce r^{C}_{SAM} [26]. When $\theta<1$ (i.e., $(P/z)^2< 1$ e.g. P= 50, z= 100 nm), predicted $r^{C}_{SAM} \approx 0.018z \approx 2$ nm. At these levels, it potentially enables patterning of lowest level vias for transistor gate lengths as short as 10 nm using 5 nm nanoparticles for contact holes. However, it does require removal of 95 nm thick resist in oxygen plasma (Figure 1 step 6) to expose 5 nm diameter GNPs.

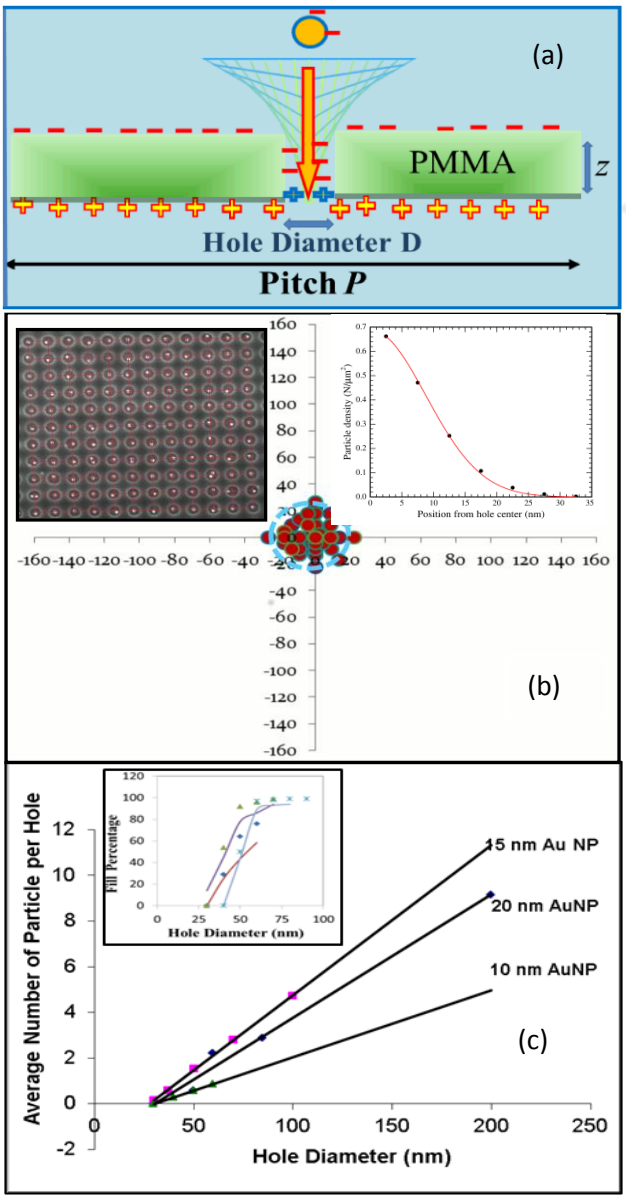

Figure 3 a) Directed deposition of NPs on patterned surfaces by electrostatic funneling. (b) NPs ($2a$= 20 nm) deposited in holes (D= 80 nm) separated by a pitch, P of 200 nm (top left inset). 93% of the holes contain one nanoparticle, and 95% of nanoparticles are within 18 nm away from the center (blue circle). Top right inset shows a Gaussian particle size placement from the center with σ= 9.0 ± 0.1 nm[27]. (c) The average number of particles deposited in holes of varying dimension shows a linear dependence with the hole diameter. (Inset) The fill fraction (f) of holes follows a Poisson statistics; $f = (1- e^{-<N>})$ where $< N >$ is the average number of particles per hole. Points (blue: 10 nm NP, green 15 nm NP, Red 20 nm NP) are experimentally determined fill fraction while the similarly colored lines were drawn using above equation.

We next consider the photoresist reflow [28-31] near the glass transition temperature of PMMA. In softened glassy state, surface tensional forces reduce curvature/roughness decreasing the effects of

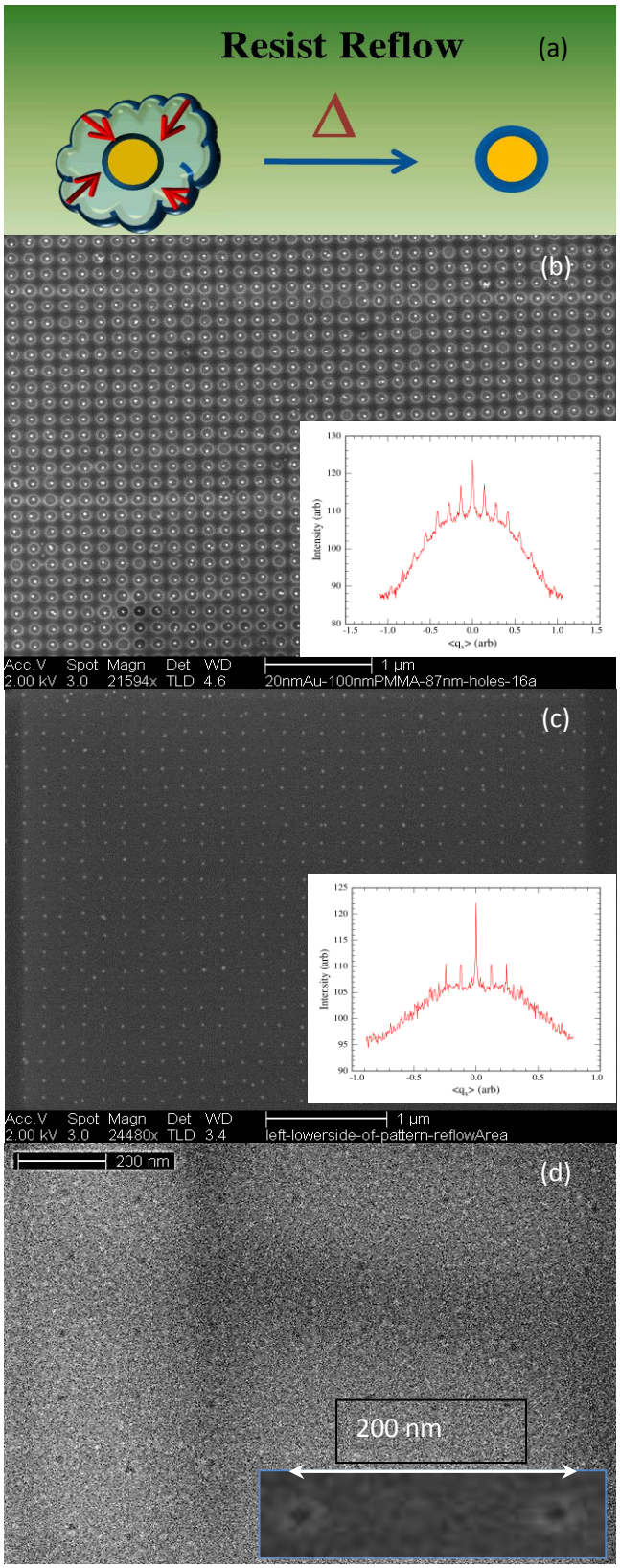

Figure 4 a) A schematic representation of resist reflow to eliminate effects of shot noise. b) SEM Image of 20 nm diameter GNPs deposited in 80 nm holes separated by 200 nm pitch. c) Image taken after resist reflow displaying nanoparticles maintain the 200 nm pitch. The insets in b and c show 2D-FTs indicating formation quasi-two dimensional crystals. d) When followed by O_2 plasma etch to expose Gold NPs, and I_2 wet etch to remove exposed GNPs, a hole pattern corresponding to deposited NPs emerges.

SN/LER as shown schematically in Figure 4a. Completely engulfing nanoparticles, as depicted in Figure 1(Step 5), is unavoidable. Thinner resist films ($z < 2a$) could be used but at the cost of nonselective NP deposition on the resist, as discussed before. One concern with the resist overflow is the possibility of dislodging GNPs by lifting them from SAM surface owing to strong capillary forces (γa, γ is surface tension), thus erasing positional registry.

Fortunately, the electrostatic forces between NPs and surface (~ $1/a^2$) are stronger, allowing for flow of polymer over the nanoparticles as depicted in Figure 4 b and c. Formation of a quasi 2D-crystal, is illustrated in the box averaged 2D-Fourier transforms presented as insets in Figures 4b and c. Exponential decrease in peak intensities is due to positional disorder of GNPs in holes (See Figure 3b). As discussed in the supplementary information, reducing this disorder would require fine tuning surface charge densities of SAM, GNP and PMMA (changing ionic strength, pH, composition etc.) to improve electrostatic funneling. Thus, after resist reflow, the hole dimension information patterned by top-down processing is erased along with the effects of SN/LER. Only the pitch information is preserved although it is affected by the particle centering uncertainty generated during NP deposition step.

GNP diameter-size holes can be recovered by light oxygen plasma etch of the resist to expose the nanoparticles followed by GNP wet-etching. Figure 4d shows crafted 20 nm size holes corresponding to the 20 nm GNP deposited in 80nm diameter holes (Figure 4b). Note the inset in Figure 4d does show line-edge roughness (≈ 5 nm) which can be reduced by thermal/solvent annealing (not shown). GNP size and final pattern contact holes had coefficient of variations (CV) of 8% and 9%(19 ± 2nm) percent respectively while our e-beam patterned 35 nm (35 ± 9) size holes shown in Figure 1 had CV of 35 percent. However, with extensive dose and focal plane optimization (which increases the processing time) we were able to reduce CV to 11 percent for 23 (23 ± 3) nm holes for e-beam-alone patterning.

Conclusions

To summarize, initial results of a new method to remove effects of shot noise in resist patterning for contact holes of sub 50 nm size are presented. The method exploits advances in synthesis of highly mono-disperse nanoparticles by using them as templates to reduce feature variance in lithographic contact hole patterning. In future, the method could be adapted to pattern other patterns such as trenches using size controlled nanowires etc. The method is limited by availability of monodisperse nanostructures and multiparticle occupancy, and misplacement with respect to hole centering, thus requiring further optimization[26].

Notes and references

[a] Chemistry Department, Portland State University, 1719 SW 10th Ave, Portland OR 97206, E-mail: ranavas@pdx.edu
[b]Portland Technology Development, Intel Corporation Ronler Acres, Hillsboro, OR 97124

† Electronic supplementary information (ESI) available: Experimental details and additional data. See DOI: 10.1039/c000000x/

1. G. E. Moore, *SPIE proceeding: Advances in Resist Technology and Processing XII*, 1995, **2438**, 2-17.
2. M. D. Levenson, N. S. Viswanathan and R. A. Simpson, *Electron Devices, IEEE Transactions on*, 1982, **29**, 1828-1836.
3. R. H. French and H. V. Tran, *Annual Review of Materials Research*, 2009, **39**, 93-126.
4. Y. Borodovsky, in *Complementary Lithography - Stochastics Suppression and EUV*, *Electronics*, *Semicon West*, San Francisco, CA 2012.
5. A. Reiser, *Photoreactive Polymers: the Science and Technology of Resists*, John Wiley & Sons, New York, 1989.
6. T. A. Brunner, *Journal of Vacuum Science & Technology B: Microelectronics and Nanometer Structures*, 2003, **21**, 2632-2637.
7. M. Krysak, A. De Silva, J. Sha, J.-K. Lee and C. K. Ober, *SPIE proceeding*, 2009, **7273**, 72732N-72732N.
8. R. Thiruvengadathan, V. Korampally, A. Ghosh, N. Chanda, K. Gangopadhyay and S. Gangopadhyay, *Reports on Progress in Physics*, 2013, **76**, 066501.
9. M. Li, R. B. Bhiladvala, T. J. Morrow, J. A. Sioss, K.-K. Lew, J. M. Redwing, C. D. Keating and T. S. Mayer, *Nat Nano*, 2008, **3**, 88-92.
10. H.-Y. Tsai, H. Miyazoe, S. Engelmann, S. Bangsaruntip, I. Lauer, J. Bucchignano, D. Klaus, L. Gignac, E. Joseph, J. Cheng, D. Sanders and M. Guillorn, *SPIE proceeding emerging patterning technology*, 2013, **8865**, 86850L-86850L.
11. Y. Lin, A. Boker, J. He, K. Sill, H. Xiang, C. Abetz, X. Li, J. Wang, T. Emrick, S. Long, Q. Wang, A. Balazs and T. P. Russell, *Nature*, 2005, **434**, 55-59.
12. C. J. Hawker and T. P. Russell, *MRS Bulletin*, 2005, **30**, 952-966.
13. J. Y. Cheng, D. P. Sanders, H. D. Truong, S. Harrer, A. Friz, S. Holmes, M. Colburn and W. D. Hinsberg, *ACS Nano*, 2010, **4**, 4815-4823.
14. H. S. P. Wong, C. Bencher, H. Yi, X.-Y. Bao and L.-W. Chang, in *Proc. SPIE 8323*, *Alternative Lithographic Technologies IV*, ed. W. M. Tong, SPIE, San Jose, 2012, pp. 832303-832303-832307.
15. Y. Chuo, C. Landrock, B. Omrane, D. Hohertz, S. V. Grayli, K. Kavanagh and B. Kaminska, *Nanotechnology*, 2013, **24**, 055304.
16. H.-W. Huang, P. Bhadrachalam, V. Ray and S. J. Koh, *Applied Physics Letters*, 2008, **93**, 073110-073110-073113.
17. L.-C. Ma, R. Subramanian, H.-W. Huang, V. Ray, C.-U. Kim and S. J. Koh, *Nano Letters*, 2007, **7**, 439-445.
18. Y. Cui, M. T. Bjork, J. A. Liddle, C. Sonnichsen, B. Boussert and A. P. Alivisatos, *Nano Letters*, 2004, **4**, 1093-1098.
19. W. Richard Bowen, A. N. Filippov, A. O. Sharif and V. M. Starov, *Advances in Colloid and Interface Science*, 1999, **81**, 35-72.
20. *The last two steps can be combined using silica nanoparticles in place of GNPs, the choice of latter was dictated by readily available commercial source, Ted Pela.* .
21. S. H. Behrens and D. G. Grier, *The Journal of Chemical Physics*, 2001, **115**, 6716-6721.
22. S. H. Brewer, W. R. Glomm, M. C. Johnson, M. K. Knag and S. Franzen, *Langmuir*, 2005, **21**, 9303-9307.
23. K. Kimura, S. Takashima and H. Ohshima, *The Journal of Physical Chemistry B*, 2002, **106**, 7260-7266.
24. C. Schonenberger, *Physical Review B*, 1992, **45**, 3861-3864.
25. C.-y. Liu and A. J. Bard, *Journal of the American Chemical Society*, 2009, **131**, 6397-6401.
26. *Please see supplementary information*.
27. *A classical Derjaguan model due to Bowen et al (see ref 19) predicts approximately Gaussian distribution as presented in supplementary information.*
28. B. C. Feng, in *US Patent 4,022,932*, International Business Machines Corporation, US, 1977, p. 5.
29. J.-H. You, J. Park, J.-M. Park, H. Jeong, J.-Y. Hong and H.-K. Oh, *Japanese Journal of Applied Physics*, 2009, **48**, 096502.
30. P. K. Montgomery, K. Lucas, K. J. Strozewski, L. Zavyalova, G. Grozev, M. Reybrouck, P. Tzviatkov and M. Maenhoudt, 2003, 807-816.
31. W. P. King, T. W. Kenny, K. E. Goodson, G. Cross, M. Despont, U. Durig, H. Rothuizen, G.

K. Binnig and P. Vettiger, *Applied Physics Letters*, 2001, **78**, 1300-1302.

Title Reducing the effects of shot noise using nanoparticles,

*Moshood K. Morakinyo,and Shankar B. Rananavare**

Removing Shot Noise. A new method is presented to remove effects of fluctuation in pattern dimensions caused by statistical variation in impinging photons/particles on nanoscale. By using precisely size controlled nanoparticles as a template in conjunction with resist reflow, the method is capable of reducing the transistor source, drain contact hole dimensions to below 20 nms and yet it is compatible with prevailing fabrication methods.